Solid-type poorly differentiated adenocarcinoma of the stomach: A characteristic morphology reveals a distinctive immunoregulatory tumor microenvironment

川床, 慎一郎

Pathology - Research and Practice 238 (2022) 154124

Contents lists available at ScienceDirect

Pathology - Research and Practice

journal homepage: www.elsevier.com/locate/prp

Solid-type poorly differentiated adenocarcinoma of the stomach: A characteristic morphology reveals a distinctive immunoregulatory tumor microenvironment

Shinichiro Kawatoko [a,b], Kenichi Kohashi [a], Takehiro Torisu [b], Taisuke Sasaki [a], Shinya Umekita [a], Eiji Oki [c], Masafumi Nakamura [d], Takanari Kitazono [b], Yoshinao Oda [a,*]

[a] Department of Anatomic Pathology, Graduate School of Medical Sciences, Kyushu University, Fukuoka, Japan
[b] Department of Medicine and Clinical Science, Graduate School of Medical Sciences, Kyushu University, Fukuoka, Japan
[c] Department of Surgery and Science, Graduate School of Medical Sciences, Kyushu University, Fukuoka, Japan
[d] Department of Surgery and Oncology, Graduate School of Medical Sciences, Kyushu University, Fukuoka, Japan

ARTICLE INFO

Keywords:
Solid-type poorly differentiated adenocarcinoma
Mismatch repair
PD-L1
IDO1

ABSTRACT

Solid-type poorly differentiated adenocarcinoma (solid-type-PDA) of the stomach is a unique histological subtype of "tubular adenocarcinoma", but little is known about its clinicopathological features, molecular pathological characteristics and immunoregulatory tumor microenvironment. Herein, we examined the immunohistochemical expressions of mismatch repair (MMR) proteins (MLH1, PMS2, MSH2, MSH6) in 57 cases of solid-type-PDA and classified them as either MMR-deficient or -proficient (dMMR, N = 23; pMMR, N = 34), and additionally identified 18 dMMR-well-differentiated adenocarcinoma (WDA) and 34 pMMR-WDA as control groups. We analyzed and compared solid-type-PDA with WDA by evaluating the immunoexpressions of key immune pathway proteins (programmed death ligand 1 (PD-L1) and indoleamine 2,3-dioxygenase 1 (IDO1)) and tumor-infiltrating lymphocytes (TILs) (CD8, Foxp3 and PD-1). The results reveled IDO1 was significantly more frequent in dMMR-solid-type-PDA than in dMMR-WDA (P = 0.0046). Moreover, dMMR-solid-type-PDA tended to have higher mean CD8+ and Foxp3+ TILs compared with dMMR-WDA [P = 0.0006 (CD8+) and P = 0.1061 (Foxp3+)], and IDO1-positive tended to be associated with a large number of CD8+, Foxp3+ or PD-1+ TILs in almost all tumor subtypes. PD-L1 was significantly observed in 44 % (15/34) of pMMR-solid-type-PDA compared with 18 % (6/34) of pMMR-WDA (P = 0.0344). Although they are molecularly and morphologically classified as the same chromosomal instability subtype, overall survival (OS) and disease-free-survival (DFS) in pMMR-solid-type-PDA were significantly worse than those in pMMR-WDA [P = 0.0216 (OS) and P = 0.0160 (DFS)]. Our study demonstrates that immunoexpressions of several immunoregulatory proteins and TILs are more prevalent in dMMR-solid-type-PDA, potentially a useful discovery for designing tumor treatments with immune checkpoint inhibitors or combination therapies with a PD-1/PD-L1-inhibitor and IDO1-inhibitor.

1. Introduction

Gastric adenocarcinoma with a predominant sheet-like growth pattern and scanty stroma is generally diagnosed as solid-type poorly differentiated adenocarcinoma (solid-type-PDA). The most recent World Health Organization classification defines solid-type-PDA as a poorly differentiated variant of "tubular adenocarcinoma" distinguishing from well/moderately differentiated tubular adenocarcinoma [1].

On the other hand, the Cancer Genome Atlas (TCGA) categorizes gastric cancers into four molecular subtypes [chromosomal instability (CIN), genomically stable (GS), microsatellite instable (MSI) and EBV-positive], a classification system that is useful for both pathological

Abbreviations: PDA, poorly differentiated adenocarcinoma; WDA, well differentiated adenocarcinoma; PD-L1, programmed death ligand 1; IDO1, indoleamine 2,3-dioxygenase 1; TILs, tumor infiltrating lymphocytes; dMMR, deficient mismatch repair; pMMR, proficient mismatch repair; MSI, microsatellite instable; OS, overall survival; PFS, progression-free survival; DFS, disease-free survival; HPD, hyperprogressive disease.

* Corresponding author at: Department of Anatomic Pathology, Graduate School of Medical Sciences, Kyushu University, Maidashi 3–1-1, Higashi-ku, Fukuoka 812-8582, Japan.
E-mail address: oda.yoshinao.389@m.kyushu-u.ac.jp (Y. Oda).

https://doi.org/10.1016/j.prp.2022.154124
Received 27 July 2022; Received in revised form 5 September 2022; Accepted 13 September 2022
Available online 15 September 2022

diagnosis and clinical treatment [2]. In addition, some studies have reported a close relationship between MSI and solid-type-PDA [3,4]. However, there is little data regarding the tumor microenvironment focused on both morphologically "solid-type" features and the above molecular subtypes. Given that solid-type-PDA represents a distinct histologic feature, we hypothesized that solid-type-PDA would have a characteristic immunoregulatory tumor microenvironment compared to that found in well-differentiated adenocarcinoma (WDA).

In recent years, the therapeutic role of immune checkpoint inhibitors has increased in several kinds of malignancy. The tumor microenvironment is increasingly emerging as an important factor in understanding tumor behaviors and predicting clinical outcomes. Programmed cell death receptor 1 (PD-1) is expressed on activated tumor-infiltrating T cell lymphocytes. Engagement with its ligand (PD-L1), expressed on the tumor cytoplasmic membrane, induces down-regulation of T cell proliferation [5] and cytokine production with induction of immunologic tolerance [6]. Indoleamine 2,3-dioxygenase 1 (IDO1) is an enzyme of L-tryptophan metabolism, and it catalyzes L-tryptophan to kynurenine [7]. Depletion of L-tryptophan causes a starvation response in cytotoxic T cells, and accumulation of kynurenine acts to hyperactivate regulatory T cells (Tregs). In the tumor microenvironment, increasing the expression of IDO1, which suppresses cytotoxic T cells and activates Tregs, enables tumor cells to acquire immunologic tolerance. IDO1 immunoexpression has been reported as a poor prognostic factor in several malignancies [8–10].

In the present study, we investigated the associations of the immunoexpression levels of PD-L1, IDO1 and tumor-infiltrating lymphocytes with clinicopathological characteristics and their prognostic value by comparing solid-type-PDA and WDA.

2. Materials and methods

2.1. Case selection

Cases were selected by reviewing written pathology reports of all 2055 gastric cancer patients diagnosed between the years 2006 and 2014 at the Department of Anatomic Pathology and searching for the keywords "poorly differentiated" and "solid". A total of 57 solid-type-PDA cases were identified based on histological examination using hematoxylin and eosin (H&E) staining. The cases were further classified into 23 deficient mismatch repair (dMMR)-solid-type-PDA and 34 proficient mismatch repair (pMMR)-solid-type-PDA based on the immunohistochemical staining of mismatch repair (MMR) proteins, as shown in the case selection flow chart (Supplementary Fig. 1 (A)).

For comparison, we additionally selected 18 dMMR-well-differentiated adenocarcinoma (WDA) and 34 pMMR-stage-match WDA from a total of 261 cases of gastric cancers resected at Kyushu University Hospital (Fukuoka, Japan) from 2012 to 2014, as shown in the control selection flow chart (Supplementary Fig. 1 (B)). All of the cancers had invaded the submucosa or beyond, and none of the patients had received preoperative chemotherapy and radiation therapy.

2.2. Histopathologic evaluation

All tumors for both groups (dMMR/pMMR-solid-type-PDA and dMMR/pMMR-WDA) were defined by applying strict morphologic criteria, described by the most recent World Health Organization classification (Fig. 1) [1] and the immunohistochemical status of MMR proteins. Solid-type-PDA had to contain sheet-like and syncytial structures consisting of medium-sized cells with vesicular nuclei and prominent nucleoli arranged in a pushing or expansile growth pattern accompanied by scant stroma and barely recognizable tubules in almost all regions of the carcinoma component. WDA was defined as having dilated or slit-like branching tubules of variable diameter. Special histological types such as hepatoid adenocarcinoma, neuroendocrine carcinoma and Epstein–Barr virus-associated gastric cancer were excluded by histological review and in situ hybridization for EBER. Patients with Lynch syndrome were also excluded. All the patients had undergone curative surgical resection. The study was approved by the Kyushu University Medical Human Investigation Committee (Institutional Review Board no. 29-354).

2.3. Clinicopathological assessment

The clinical characteristics of all cases were analyzed, including patient age and sex, tumor location, tumor size, invasion depth, lymph node metastasis, lymphatic permeation and venous invasion. All patients were staged according to the 8th edition of the Union for International Cancer Control (UICC) TNM classification.

2.4. Immunohistochemical assessment and scoring

For all cases, formalin-fixed, paraffin-embedded tumor tissues were sliced into 3 μm-thick sections, and immunohistochemical staining was performed using the universal immunoperoxidase polymer method (Envision-kit and Envision Flex-kit; Dako, Tokyo). Antigen retrieval was carried out by heating the slides in 10 mM sodium citrate (pH 6.0), Target Retrieval Solution (Dako, Carpinteria, CA) or ethylenediaminetetraacetic acid. Supplementary Table 1 summarizes the primary antibodies and staining conditions utilized in this study.

The expressions of MLH1, PMS2, MSH2 and MSH6 were judged as "deficient" when there was a complete absence of nuclear staining in tumor cells, while the surrounding lymphocytes, fibrocytes and vascular endothelial cells showed consistently preserved nuclear staining. A

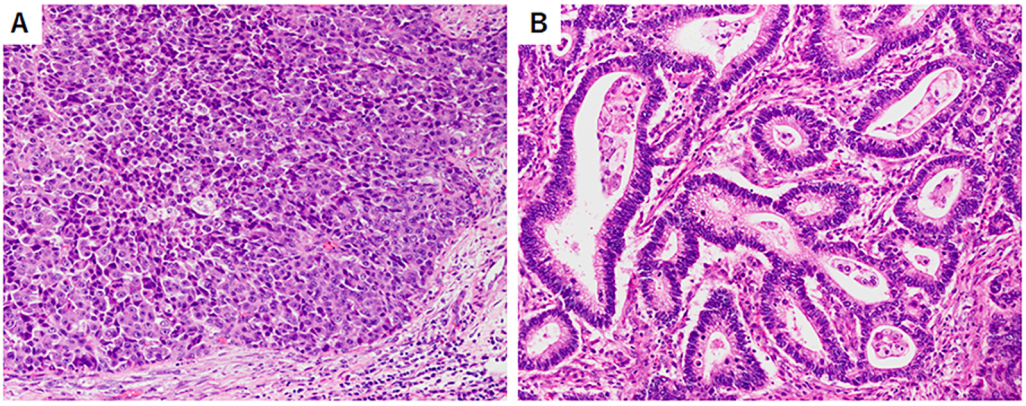

Fig. 1. Histomorphology of gastric cancers on hematoxylin and eosin (H&E) staining. A, solid-type-PDA is characterized by a sheet-like and syncytial growth pattern accompanied by scant stroma and barely recognizable tubules. B, WDA is defined as having dilated or slit-like branching tubules of variable diameters.

representative immunohistochemical staining pattern of MMR deficiency is shown in Supplementary Fig. 2. When the tumor cells demonstrated the proficient immunohistochemical expression of all four MMR proteins, the tumor could be considered microsatellite stable (pMMR-tumor). When the tumor displayed deficient immunohistochemical expression of one or more MMR proteins, the tumor was considered likely to have microsatellite instability (dMMR-tumor).

Immune staining for PD-L1 was scored as positive when the combined positive score (CPS) ≥1 % (CPS = [(number of PD-L1-positive tumor cells, -lymphocytes and -macrophages) / (total number of tumor cells)] × 100), as reported in the literature [11], and was further subdivided by extent as 1–5 % or >5 %. PD-L1 exhibits cytoplasmic membrane staining. The IDO1 result was defined based on the tumor proportion score (TPS) (TPS = [(number of IDO1-positive tumor cells) / (total number of tumor cells)] × 100). Cytoplasmic IDO1 TPS ≥1 % was considered positive [12]. In addition, we identified the extent of staining as 1–50 % or >50 % of cells.

Intraepithelial and stromal lymphocytes positive for CD8, Foxp3, and PD-1 were manually counted under 400 × magnification at the deepest invasive front of five independent fields in the cancer tissue, and the mean score was set as the final expression score [12].

All microscopic immunohistochemical staining results for each sample were independently evaluated by three pathologists (S.K., K.K., and Y.O.) in the absence of clinical data. Immunohistochemical images are shown in Fig. 2.

2.5. In situ hybridization of Epstein-Barr virus-encoded small RNA (EBER)

To detect Epstein-Barr virus (EBV) infection, we stained 3 μm-thick sections for in situ hybridization according to the manufacturer's instructions. The EBER probe (#Y5200, Dako) was detected using a PNA ISH Detection Kit (#K5201, Dako). Only cases with a strong signal within more than 95 % of tumor cell nuclei were interpreted as positive.

2.6. Assessment for MSI by polymerase chain reaction (PCR)

Since immunohistochemical staining using four MMR antibodies against MLH1, PMS2, MSH2, and MSH6 has been shown to be a sensitive surrogate marker for distinguishing dMMR from pMMR-tumors [13], we carried out PCR solely on deficient MMR-tumors (23 solid-type-PDA cases and 18 WDA cases). Microsatellite status was assessed by analyzing DNA extracted from formalin-fixed, paraffin-embedded tumor tissue sections using an MSI Analysis Kit (FALCO) (FALCO biosystems) with five mononucleotide repeat markers (BAT25, BAT26, NR21, NR24 and MONO27) according to the methodology previously reported [14]. PCR was performed by a Veriti thermal cycler (Life Technologies), and the PCR amplicon was diluted by distilled water and applied to a 3130xl Genetic Analyzer (Life Technologies). Fragment analysis was carried out using GeneMapper software (Life Technologies). Tumors exhibiting markers outside the corresponding QMVR were defined as MSI. We classified microsatellite instability at ≥ 2 mononucleotide loci as

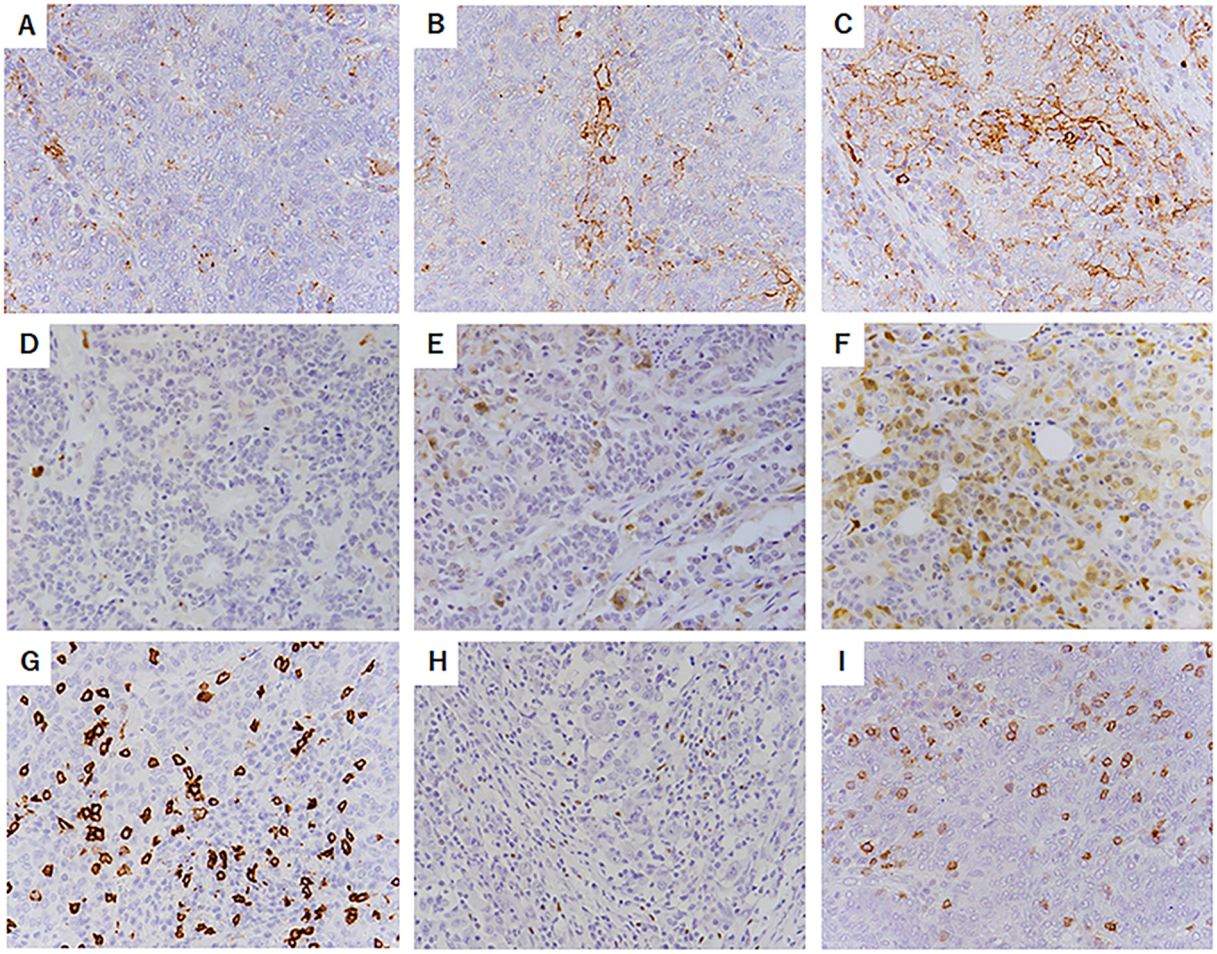

Fig. 2. Expressions of PD-L1, IDO1 and TILs. A-F, representative images of the immunoexpressions of PD-L1 (A, PD-L1 CPS<1 %; B, 1–5%; C, >5 %) and IDO1 (D, IDO1 TPS<1 %; E, 1–50 %; F, >50 %) in solid-type-PDA. PD-L1 membrane staining and IDO1 cytoplasmic staining were observed. G-I, representative images of TILs at the invasive front in solid-type-PDA (G, CD8; H, Foxp3; I, PD-1).

MSI-high, instability at one mononucleotide locus as MSI-low, and no instability at any of the loci as microsatellite stable (MSS).

2.7. Statistical analysis

All statistical analyses were performed using the JMP Statistical Discovery Software (version 14.0; SAS, Cary, NC). Fisher's exact test was used to investigate the correlation between two dichotomous variables with respect to clinicopathological features and expression of PD-L1, IDO1 or TILs (CD8, Foxp3, and PD-1). The correlation between PD-L1 or IDO1 expression and TILs was calculated by Wilcoxon's test. Overall survival (OS) was defined as the time from surgery to the time of last follow-up or death from gastric cancer, and progression-free-survival (PFS) was defined as the time from surgery to the date when a new lymph node or distal metastasis was detected or the last follow-up. Excluding 4 cases diagnosed as pathological Stage IV at the time of surgery, disease-free-survival (DFS) was defined in the same way as PFS. All survival data were calculated using the Kaplan-Meier method, and differences were evaluated by the log-rank test. All tests were two-sided with 0.05 as the threshold P-value indicating statistical significance.

3. Results

3.1. Clinicopathological characteristics, immunohistochemistry of MMR proteins and microsatellite status

The clinicopathological characteristics and the results of immunohistochemistry of MMR proteins are summarized in Table 1 and Supplementary Tables 2 and 3. A total of 109 cases were identified, and cases were classified into four subtypes based on morphological features and MMR expression status: dMMR-solid-type-PDA (N = 23), dMMR-WDA (N = 18), pMMR- solid-type-PDA (N = 34) and pMMR-WDA (N = 34). All 41 MMR-deficient tumors showed a concurrent loss of MLH1/PMS2; none of the cases showed other patterns of MMR deficiency. After excluding the 9 dMMR tumors with insufficient quality of DNA or level of PCR amplification, MSI analysis revealed that all 32 of the remaining MMR-deficient tumors were MSI-High.

The comparison of solid-type-PDA and WDA for each group (dMMR or pMMR) revealed that solid-type-PDA was larger at presentation than WDA [P = 0.0110 (dMMR) or P = 0.0490 (pMMR)] and tended to present at higher pT stages compared to WDA [P = 0.0122 (dMMR) or P = 0.3053 (pMMR)]. Venous invasion was frequently seen in the solid-type-PDA [P = 0.2911 (dMMR) or P = 0.1435 (pMMR)].

As for the comparison of dMMR and pMMR tumors, dMMR status was significantly related with older age, female predominance and lower third location, consistent with a previous study (Supplementary Table 3) [3].

3.2. PD-L1 expression differs among tumor subtypes

PD-L1 membranous expression was observed in dMMR-solid-type-PDA (65 %: 15/23), dMMR-WDA (56 %: 10/18), pMMR-solid-type-PDA (44 %: 15/44) and pMMR-WDA (18 %: 6/34) (Fig. 3 (A)). PD-L1 expression was significantly more frequent in pMMR-solid type-PDA than in pMMR-WDA (P = 0.0344). There was no significant difference between dMMR-solid-type-PDA and dMMR-WDA (P = 0.7477), but PD-L1 overexpression (>5 %) was found more frequently in dMMR-solid-type-PDA (17 %: 4/23) than in dMMR-WDA (6 %: 1/18).

3.3. IDO1 expression differs among tumor subtypes

IDO1 immunostaining was detected in the cytoplasm of tumor cells in dMMR-solid-type-PDA (91 %: 21/23), dMMR-WDA (50 %: 9/18), pMMR-solid-type-PDA (44 %: 15/34) and pMMR-WDA (32 %: 11/34) (Fig. 3 (B)). dMMR-solid-type-PDA showed significantly more frequent expression of IDO1 than dMMR-WDA (P = 0.0046). Notably, IDO1 overexpression (>50 %) was markedly more prevalent in dMMR-solid-type-PDA (52 %: 12/23) than in dMMR-WDA (6 %: 1/18), pMMR-solid-type-PDA (12 %: 4/34) or pMMR-WDA (0 %: 0/34).

3.4. TILs (CD8+, Foxp3+ and PD-1+) density differ among tumor subtypes

Absolute and mean counts for tumor-infiltrating lymphocytes are summarized in Fig. 4. The mean CD8+ lymphocyte count in dMMR-solid-type-PDA was higher than that in dMMR-WDA (P = 0.0006). As for Foxp3+ lymphocytes in the dMMR and pMMR groups, although the difference was not significant, solid-type-PDA tended to contain higher numbers of Foxp3+ lymphocytes than WDA [P = 0.1061 (dMMR) or P = 0.8540 (pMMR)]. A subgroup analysis comparing PD-1+ lymphocytes between solid-type-PDA and WDA in both dMMR and pMMR groups revealed no statistically significant differences.

In both solid-type-PDA and WDA tumors, dMMR-tumors significantly contained higher numbers of CD8+ and Foxp3+ TILs compared with pMMR-tumors in spite of the same histology [solid-type-PDA; P < 0.0001 (CD8+) or P = 0.0030 (Foxp3+) / WDA; P = 0.0013 (CD8+) or P = 0.0387 (Foxp3+)].

Table 1
Clinicopathologic characteristics of gastric cancers (N = 109): comparative study of solid-type PDA and WDA tumors.

		dMMR group (N=41)		P value	pMMR group (N=68)		P value
		solid-type PDA (N=23)	WDA (N=18)		solid-type PDA (N=34)	WDA (N=34)	
Age (years; median, range)		76.7 (62–90)	77.9 (67–88)	1.0000	71.6 (55–87)	69.9 (57–85)	0.6205
Sex	Male	10 (43 %)	11 (61 %)	0.3499	27 (79 %)	27 (79 %)	1.0000
	Female	13 (57 %)	7 (39 %)		7 (21 %)	7 (21 %)	
Location	Upper	3 (13 %)	2 (11 %)	0.7273	7 (20 %)	11 (32 %)	0.5067
	Middle	6 (26 %)	3 (17 %)		19 (56 %)	15 (44 %)	
	Lower	14 (61 %)	13 (72 %)		8 (24 %)	8 (24 %)	
Size (mm; median, range)		78.6 (18–140)	44.9 (15–70)	0.0110[a]	76.1 (12–170)	49.9 (10–92)	0.0490[a]
pT stage	pT1b (SM)	2 (9 %)	8 (44 %)	0.0122[a]	3 (9 %)	5 (15 %)	0.3053
	pT2 (MP)	5 (21 %)	5 (28 %)		6 (18 %)	9 (26 %)	
	pT3 (SS)	13 (57 %)	4 (22 %)		15 (44 %)	12 (35 %)	
	pT4a,4b (SE,SI)	3 (13 %)	1 (6 %)		10 (29 %)	8 (24 %)	
Lymph node metastasis (+)		14 (61 %)	6 (33 %)	0.1180	23 (68 %)	28 (82 %)	0.2624
Lymphatic permeation (+)		15 (65 %)	12 (67 %)	1.0000	18 (53 %)	22 (65 %)	0.4601
Venous invasion (+)		8 (35 %)	3 (17 %)	0.2911	22 (65 %)	15 (44 %)	0.1435
Pathological stage	stage IA-IIB	14 (61 %)	16 (89 %)	0.0753	18 (53 %)	18 (53 %)	1.0000
	stage IIIA-IV	9 (40 %)	2 (11 %)		16 (47 %)	16 (47 %)	

[a] Significant difference.

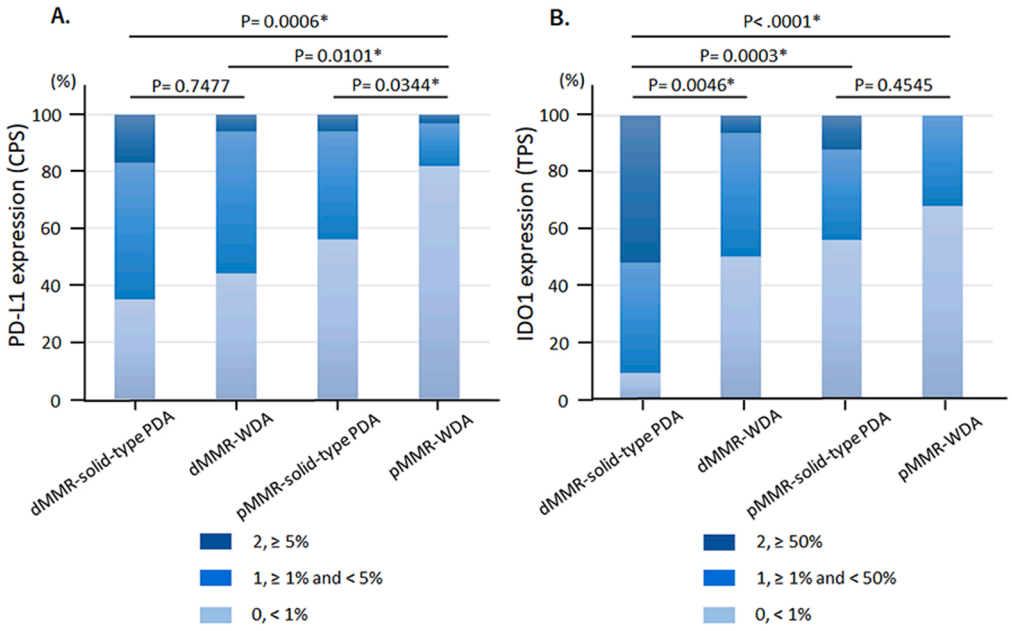

Fig. 3. The percentages of tumor proportion scores were as follows: PD-L1 (0, < 1 %; 1, ≥1 % and <5 %; 2, ≥5 %); IDO1 (0, < 1 %, 1, ≥1 % and < 50 %; 2, ≥50 %). Correlations of the immunoexpression of PD-L1 (A) and IDO1 (B) with each tumor subtype are shown.

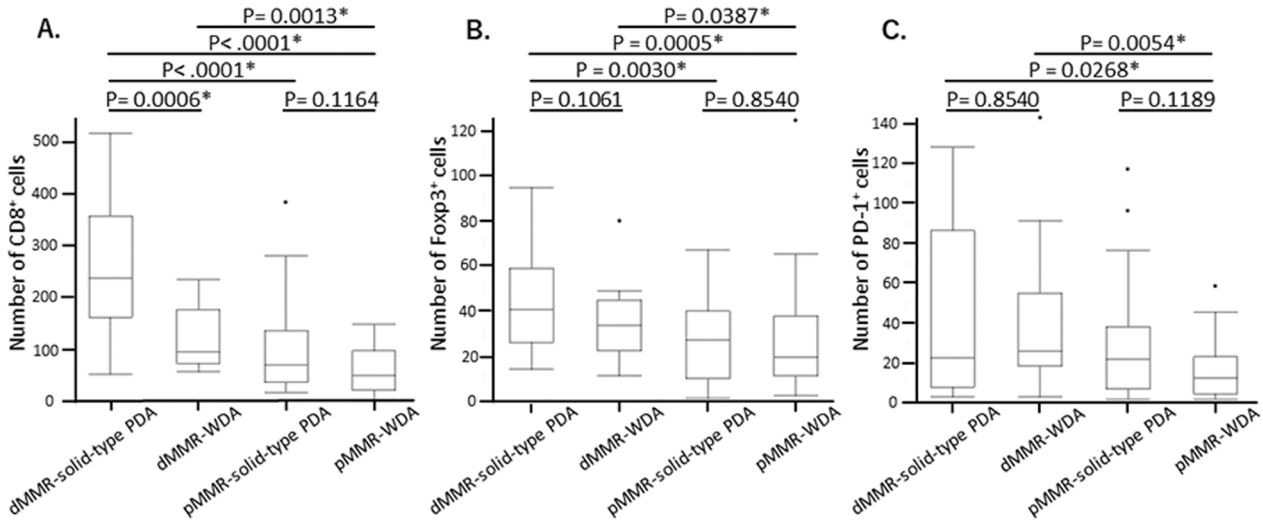

Fig. 4. Comparisons of TILs (A, CD8+; B, Foxp3+ and C, PD-1+) among tumor subtypes.

3.5. Relationship between PD-L1/IDO1 expression and TILs density

We evaluated the correlations of PD-L1/IDO1 expression with TILs (CD8+, Foxp3+ and PD-1+) for each tumor subtype (Fig. 5a, b). As for dMMR-solid-type-PDA or pMMR-solid-type-PDA, PD-L1-positive cases had significantly higher infiltration rates of CD8+ TILs than equivalent PD-L1-negative cases [P = 0.0061 (dMMR-solid-type-PDA), P = 0.0061 (pMMR-solid-type-PDA)] (Fig. 5a (A,C)). No significant relationship was observed between PD-L1 expression and Foxp3+ TILs in all tumor subtypes (Fig. 5a (E-H)). In dMMR-solid-type-PDA alone, PD-L1 expression showed a strong relationship with PD-1+ TILs (P = 0.0329) (Fig. 5a (I)).

As for dMMR-solid-type-PDA and both pMMR groups (solid-type-PDA and WDA), TILs (CD8+ and Foxp3+) were significantly more frequent in IDO1-positive cases than in IDO1-negative cases (Fig. 5b, (A, C,D,E,G,H)). IDO1 expression was significantly related to a high number of PD-1+ TILs in the pMMR group [P = 0.0037 (solid-type-PDA), P = 0.0002 (WDA)] (Fig. 5b, (K,L)).

3.6. Prognosis after surgery

We assessed the prognostic significance of histological features, microsatellite status, PD-L1/IDO1 expression and TILs (CD8+, Foxp3+ and PD-1+) using Kaplan-Meier survival analysis. In the pMMR group, OS and DFS were significantly worse in solid-type-PDA than in WDA despite stage-matching [P = 0.0216 (OS), P = 0.0160 (DFS)] (Fig. 6, (D,F)). In the dMMR group, WDA showed relatively longer overall survival than solid-type-PDA, but the difference did not reach significance (P = 0.3834) (Fig. 6, (A)). In comparisons of dMMR and pMMR with regard to each histological feature, the prognosis of dMMR was significantly better than that of pMMR (Supplementary Fig. 3). In our present study, there were no significant correlations between

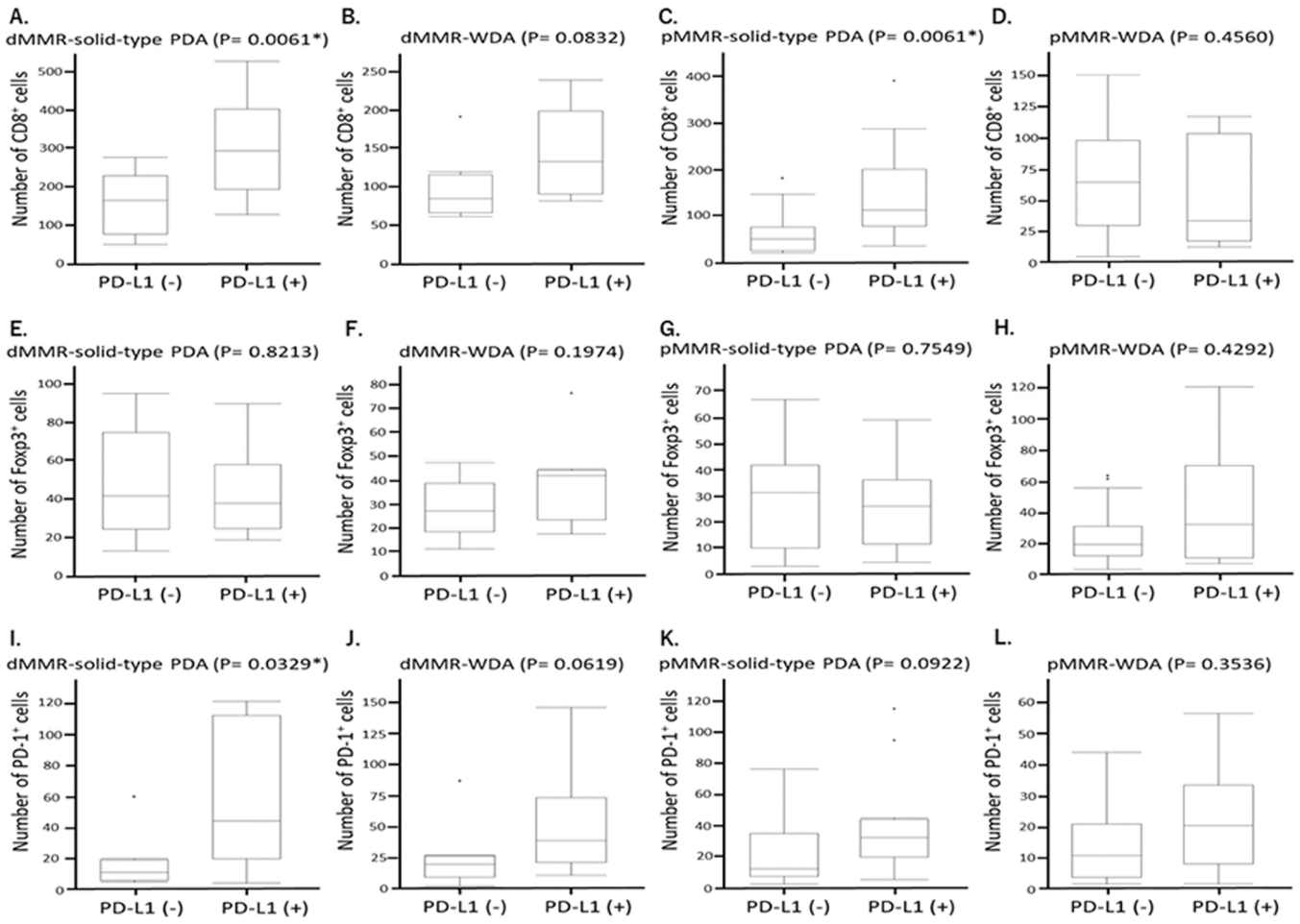

Fig. 5a. The correlations of TILs (CD8+, Foxp3+ and PD-1+) with the immunoexpression of PD-L1 for each tumor subtype. A-D, PD-L1 expression and CD8+ TILs. E-H, PD-L1 expression and Foxp3+ TILs. I-L, PD-L1 expression and PD-1+ TILs.

immunohistochemical status and prognosis for any tumor subtype (Supplementary Fig. 4). PD-L1/IDO1 expression and the level of TILs (CD8+, Foxp3+ and PD-1+) were not significant prognostic markers in these tumor subtypes.

4. Discussion

In the expression of immunoregulatory proteins and the tumor microenvironment, we focused on the distinctive histological feature "solid structure" and classified the cases into deficient MMR or proficient MMR in accordance with the four molecular subtypes proposed by TCGA [2]. In our present study, PD-L1 and IDO1 expression in dMMR-solid-type-PDA were respectively observed in 15 cases (65 %) and 21 cases (91 %). These prevalence rates were higher than those for other molecular subtypes and those reported in previous research, with PD-L1 and IDO1 expressions at 59 % [15] and 50 % [16] in non-sorted/broad gastric cancers. Notably, we also confirmed that infiltration of CD8+ cytotoxic T cells and Foxp3+ Tregs was found significantly more frequently in dMMR-solid-type-PDA than in the other tumor subtypes. IDO1-positive expression tended to be associated with a large number of CD8+, Foxp3+ or PD-l+ TILs in almost all tumor subtypes. These results suggested that treatment with immune checkpoint inhibitors may be effective for dMMR-solid-type-PDA.

PD-1/PD-L1 blockades induce recovery of dysfunctional CD8+ cytotoxic T cells [17]. They also enhance Foxp3+ Tregs-mediated immunosuppression because of the high PD-1 expression in Tregs [18]. Kamada et al. compared gastric cancer tumor samples before and after PD-1 blockade therapy and revealed that this treatment notably increased tumor-infiltrating proliferative Tregs in samples from hyper-progressive disease (HPD) patients who experienced rapid cancer progression after PD-1/PD-L1 blockade therapy, as opposed to reducing Tregs in samples of non-HPD patients [19]. PD-1/PD-L1 blockade promotes the proliferation of highly suppressive PD-1+ Tregs in HPD patients and may result in the inhibition of antitumor immunity. Therefore, suppression of Tregs is important for antitumor effects in the PD1/PD-L1 blockade.

IDO1 plays a major role in tumor immunology and is a potential immune-based therapeutic target [10]. IDO1 inhibition reduces Tregs and promotes the proliferation of effector T cells. In our present study, there was a significant correlation between IDO1 immunopositivity and high numbers of infiltrating CD8+ cytotoxic T cells and Foxp3+ Tregs in almost all tumor subtypes of gastric cancer regardless of microsatellite status. Therefore, IDO1 inhibition in gastric cancer patients may also enhance antitumor effects by suppressing Tregs. Our present results suggested that combination therapy targeting PD-L1 and IDO1 might improve the poor outcome of advanced gastric cancers, especially for the patients acquiring immune tolerance via the IDO1-immunosuppressive pathway, such as dMMR-solid-type-PDA. Indeed, in clinical studies, the combination of PD-1/PD-L1 and IDO1 inhibitors has already shown potential for use in the treatment of other malignancies [8,9].

We investigated the prognostic significance of immunohistochemical results, but no significant relation was detected. The effects of PD-L1/IDO-1 expression and TILs on the prognosis of gastric cancers have been controversial; prior studies have reported that IDO1 as associated with poor prognosis [20,21] whereas high levels of visual TIL estimates and Foxp3+ TILs were markedly associated with increased overall

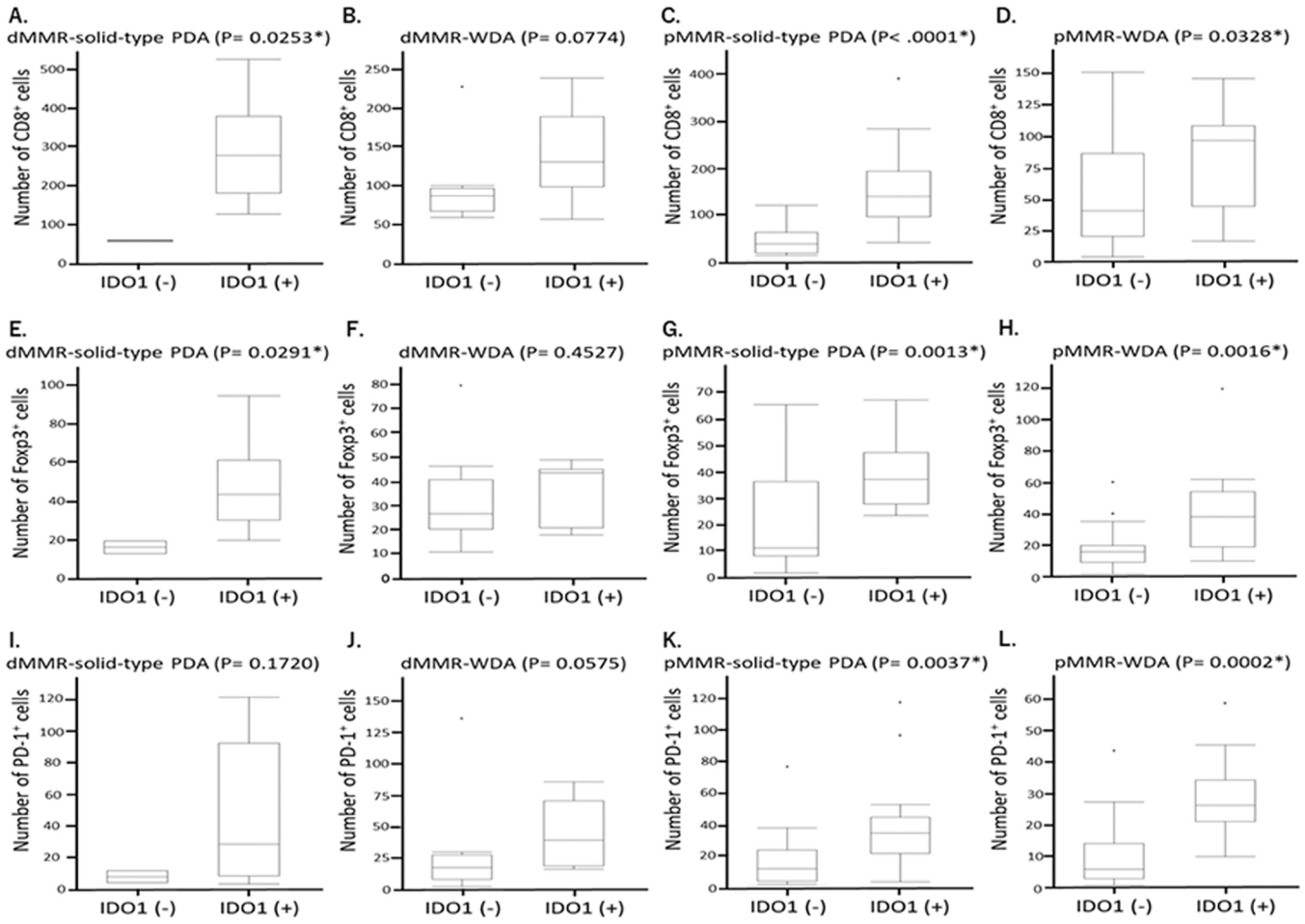

Fig. 5b. The correlations of TILs (CD8+, Foxp3+ and PD-1+) with the immunoexpression of IDO1 for each tumor subtype. A-D, IDO1 expression and CD8+ TILs. E-H, IDO1 expression and Foxp3+ TILs. I-L, IDO1 expression and PD-1+ TILs.

survival [22]. In other malignancies, both PD-L1 expression [23] and IDO1 expression [8–10] have been associated with worse prognosis. For accurate prognosis estimation, it is necessary to categorize a large number of gastric cancer cases both molecularly and morphologically, and then analyze the prognosis for each subtype.

We also represented that dMMR-tumors significantly contained higher numbers of CD8+ and Foxp3+ TILs compared with pMMR-tumors regardless histological feature, consistent with a previous research [16]. Some studies have reported that dMMR-tumors have a high frequency of somatic mutations rather than pMMR-tumors because of the functional deficiency in MMR proteins [24]. As the genetic mutations result in 'neoantigen' production and TILs are activated upon presentation of these antigens, dMMR-tumors frequently have higher mean TILs compared with pMMR-tumors.

As for the clinicopathological features, in the pMMR groups, solid-type-PDA had a significantly worse prognosis than WDA despite stage-matching. According to the WHO classification [1], solid-type-PDA is classified as the poorly differentiated variant of "tubular adenocarcinoma", which is the same category as WDA (i.e., the well-differentiated variant of "tubular adenocarcinoma"). Both variants of tubular adenocarcinoma correspond to the intestinal-type histology in Lauren's classification [25]; according to the four molecular subtypes proposed by TCGA [2], they are collectively classified as chromosomal instability (CIN) based on mismatch repair proficiency. Although they are categorized in the same subtype molecularly and morphologically, the specific histological feature "solid-type" should be classified as a prognostic histological finding.

In our present study, all 32 gastric cancer cases determined to be MMR deficient by immunohistochemical staining, excluding the 9 cases with poor DNA quality, showed MSI-High by PCR analysis using the five mononucleotide repeat markers. Furthermore, all 41 MMR-deficient gastric cancers showed concurrent loss of MLH1/PMS2, and none of the cases showed other patterns of MMR deficiency, such as isolated PMS2 deficiency, concurrent MSH2/MSH deficiency and isolated MSH6 deficiency. Almost all sporadic gastric cancers with dMMR have been reported to show concurrent loss of MLH1/PMS2 [26], which is consistent with our present results. In addition, approximately 95 % of microsatellite instability-high cancer has been reported to exhibit a loss of MMR protein immunoexpression [27]. In sporadic gastric cancer, immunohistochemistry of MLH1/PMS2 may be useful as a surrogate marker of high microsatellite instability. This surrogate marker can play an important role in determining treatment strategies when PCR cannot be performed due to the low tumor cell percentage, such as from biopsy specimens or after chemotherapy.

The prognosis of gastric cancers with mismatch repair deficiency has been better than that of mismatch repair proficiency [28]. Similarly, in our present study, dMMR status was associated with better overall survival than pMMR status in both solid-type-PDA and WDA tumors. Therefore, the MMR status in gastric cancer is a beneficial biomarker of prognostic evaluation. However, some clinical trials showed that a defective mismatch repair might be a predictive marker for lack of efficacy of standard adjuvant chemotherapy (fluoropyrimidine + platinum) in advanced gastric cancer [29]. MMR components are required for the induction of apoptosis by many DNA-damaging agents, and the MMR complex hMutS alpha specifically recognizes and binds to 5-FU-modified DNA [30]. Therefore, a gastric cancer patient with MSI-H

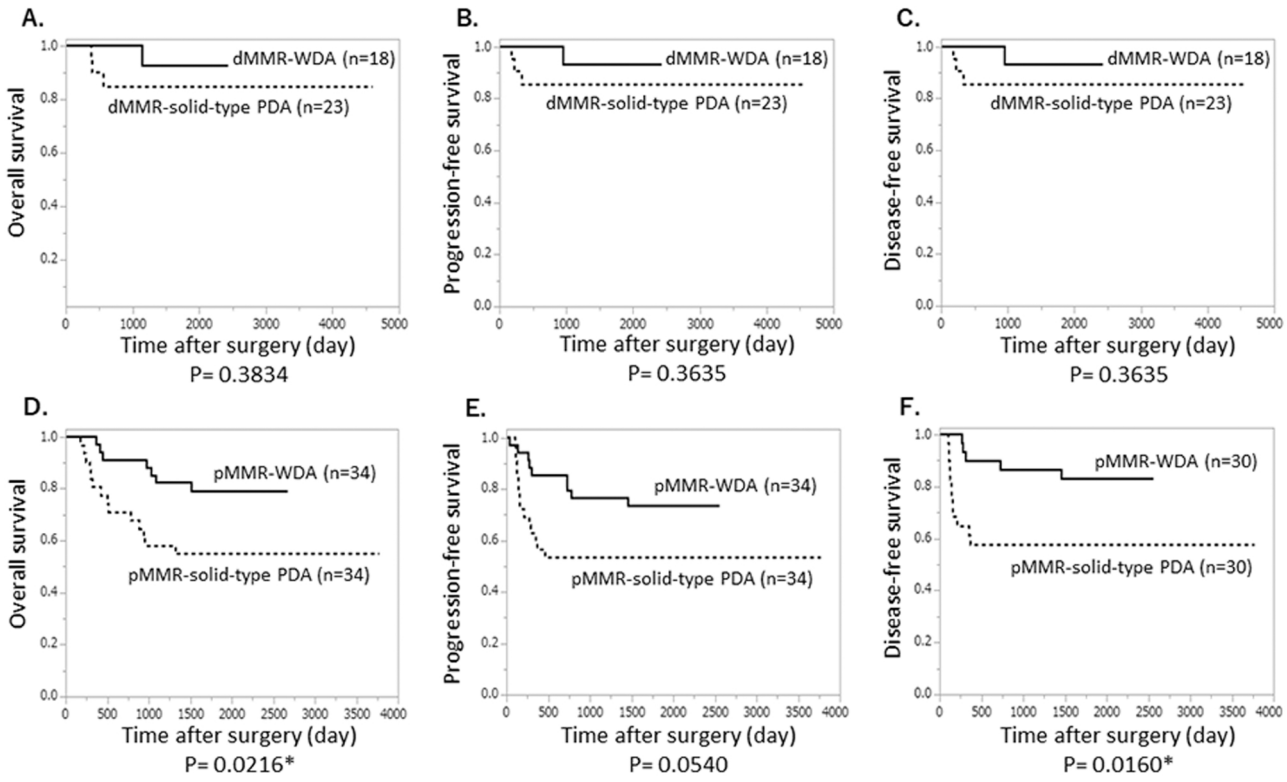

Fig. 6. Kaplan-Meier curves of overall survival, progression-free-survival and disease-free-survival according to histological features (log-rank test). Each microsatellite status was compared between solid-type-PDA and WDA (dMMR (A-C) and pMMR (D-F)).

is considered to have low drug sensitivity, which has also been observed in advanced colorectal cancer patients with MSI-H [31]. Although routine evaluation for MSI status is not recommended according to the most recent World Health Organization guidelines [1], it is worth considering whether mispatch repair deficiency is present when selecting adjuvant chemotherapy. We think that the evaluation of MMR status may be important not only to determine prognosis, but also for drug selection, including the decision to use immune checkpoint inhibitors.

The limitation in our study was the different time periods covered between solid-type-PDA and WDA, which is difficult to compare prognostic curves.

In conclusion, we investigated PD-L1 and IDO1 expressions and TILs status in solid-type-PDA compared to WDA. We have shown that the tumor microenvironment of dMMR-solid type-PDA represents a complex balance between a pro-inflammatory antitumor response and immune regulation via immune checkpoint inhibition. IDO1 expression was frequently observed in dMMR-solid-type-PDA, and IDO1 expression was associated with a high density of TILs. This study also suggests that combination therapy with a PD-1/PD-L1 inhibitor and an IDO1 inhibitor may be effective for treating dMMR-solid-type-PDA to avoid hyperprogressive disease.

Compliance with ethical standards

This study was conducted in accordance with the principles embodied in the Declaration of Helsinki. The study was approved by the Ethics Committee of Kyushu University (No. 29–354). Informed consent was obtained from the subjects or guardians.

CRediT authorship contribution statement

S. Kawatoko performed the research and wrote the paper. K. Kohashi, T. Torisu, T. Sasaki, S. Umekita, E. Oki, and M. Nakamura contributed to the research design and slide review. T. Kitazono and Y. Oda designed the research and gave final approval of the manuscript. All authors critically reviewed and approved the manuscript.

Declaration of Competing Interest

All authors declare that they have no conflicts of interest to disclose.

Acknowledgments

We appreciated the technical assistance from The Research Support Center, Kyushu University Graduate School of Medical Sciences. The English in this manuscript was revised by KN International (https://www.kninter.co.jp/).

Appendix A. Supporting information

Supplementary data associated with this article can be found in the online version at doi:10.1016/j.prp.2022.154124.

References

[1] F. Carneiro, M. Fukayama, H.I. Grabsch, W. Yasui, Gastric adenocarcinoma. The WHO classification of tumours editorial board eds. WHO classification of tumours. Digestive System Tumours, 5th edition, IARC Press, Lyon, France, 2019, pp. 85–95.
[2] N. Cancer Genome Atlas Research, Comprehensive molecular characterization of gastric adenocarcinoma, Nature 513 (2014) 202–209.
[3] S. Tsuruta, K. Kohashi, Y. Yamada, M. Fujiwara, Y. Koga, E. Ihara, Y. Ogawa, E. Oki, M. Nakamura, Y. Oda, Solid-type poorly differentiated adenocarcinoma of the stomach: Deficiency of mismatch repair and SWI/SNF complex, Cancer Sci. 111 (2020) 1008–1019.
[4] T. Arai, Y. Matsuda, J. Aida, K. Takubo, T. Ishiwata, Solid-type poorly differentiated adenocarcinoma of the stomach: clinicopathological and molecular characteristics and histogenesis, Gastric Cancer 22 (2019) 314–322.
[5] G.J. Freeman, A.J. Long, Y. Iwai, K. Bourque, T. Chernova, H. Nishimura, L.J. Fitz, N. Malenkovich, T. Okazaki, M.C. Byrne, H.F. Horton, L. Fouser, L. Carter, V. Ling, M.R. Bowman, B.M. Carreno, M. Collins, C.R. Wood, T. Honjo, Engagement of the PD-1 immunoinhibitory receptor by a Novel B7 family member leads to negative regulation of lymphocyte activation, J. Exp. Med 192 (2000) 1027–1034.

[6] M.E. Keir, M.J. Butte, G.J. Freeman, A.H. Sharpe, PD-1 and its ligands in tolerance and immunity, Annu Rev. Immunol. 26 (2008) 677–704.
[7] C. Uyttenhove, L. Pilotte, I. Theate, V. Stroobant, D. Colau, N. Parmentier, T. Boon, B.J. Van den Eynde, Evidence for a tumoral immune resistance mechanism based on tryptophan degradation by indoleamine 2,3-dioxygenase, Nat. Med. 9 (2003) 1269–1274.
[8] Y. Kozuma, K. Takada, G. Toyokawa, K. Kohashi, M. Shimokawa, F. Hirai, T. Tagawa, T. Okamoto, Y. Oda, Y. Maehara, Indoleamine 2,3-dioxygenase 1 and programmed cell death-ligand 1 co-expression correlates with aggressive features in lung adenocarcinoma, Eur. J. Cancer 101 (2018) 20–29.
[9] L. Zhai, E. Ladomersky, K.L. Lauing, M. Wu, M. Genet, G. Gritsina, B. Gyorffy, P. K. Brastianos, D.C. Binder, J.A. Sosman, F.J. Giles, C.D. James, C. Horbinski, R. Stupp, D.A. Wainwright, Infiltrating T cells increase IDO1 expression in glioblastoma and contribute to decreased patient survival, Clin. Cancer Res. 23 (2017) 6650–6660.
[10] Y. Kiyozumi, Y. Baba, K. Okadome, T. Yagi, T. Ishimoto, M. Iwatsuki, Y. Miyamoto, N. Yoshida, M. Watanabe, Y. Komohara, H. Baba, IDO1 expression is associated with immune tolerance and poor prognosis in patients with surgically resected esophageal cancer, Ann. Surg. 269 (2019) 1101–1108.
[11] S. Ahn, K.M. Kim, PD-L1 expression in gastric cancer: interchangeability of 22C3 and 28-8 pharmDx assays for responses to immunotherapy, Mod. Pathol. 34 (2021) 1719–1727.
[12] K. Friedman, A.S. Brodsky, S. Lu, S. Wood, A.J. Gill, K. Lombardo, D. Yang, M. B. Resnick, Medullary carcinoma of the colon: a distinct morphology reveals a distinctive immunoregulatory microenvironment, Mod. Pathol. 29 (2016) 528–541.
[13] H. Hampel, W.L. Frankel, E. Martin, M. Arnold, K. Khanduja, P. Kuebler, H. Nakagawa, K. Sotamaa, W. Thomas, J. Westman, J. Panescu, D. Fix, J. Lockman, I. Comeras, A. Chapelle, Screening for the lynch syndrome (Hereditary Nonpolyposis Colorectal Cancer), N. Engl. J. Med. 352 (2005) 1851–1860.
[14] H. Bando, W. Okamoto, T. Fukui, T. Yamanaka, K. Akagi, T. Yoshino, Utility of the quasi-monomorphic variation range in unresectable metastatic colorectal cancer patients, Cancer Sci. 109 (2018) 3411–3415.
[15] X. Liu, M.G. Choi, K. Kim, K.M. Kim, S.T. Kim, S.H. Park, R. Cristescu, S. Peter, J. Lee, High PD-L1 expression in gastric cancer (GC) patients and correlation with molecular features, Pathol. Res. Pr. 216 (2020), 152881.
[16] P.A. Patil, A.M. Blakely, K.A. Lombardo, J.T. Machan, T.J. Miner, L.J. Wang, A. S. Marwaha, A. Matoso, Expression of PD-L1, indoleamine 2,3-dioxygenase and the immune microenvironment in gastric adenocarcinoma, Histopathology 73 (2018) 124–136.
[17] L.M. Francisco, V.H. Salinas, K.E. Brown, V.K. Vanguri, G.J. Freeman, V. K. Kuchroo, A.H. Sharpe, PD-L1 regulates the development, maintenance, and function of induced regulatory T cells, J. Exp. Med. 206 (2009) 3015–3029.
[18] S. Kumagai, Y. Togashi, T. Kamada, E. Sugiyama, H. Nishinakamura, Y. Takeuchi, K. Vitaly, K. Itahashi, Y. Maeda, S. Matsui, T. Shibahara, Y. Yamashita, T. Irie, A. Tsuge, S. Fukuoka, A. Kawazoe, H. Udagawa, K. Kirita, K. Aokage, G. Ishii, T. Kuwata, K. Nakama, M. Kawazu, T. Ueno, N. Yamazaki, K. Goto, M. Tsuboi, H. Mano, T. Doi, K. Shitara, H. Nishikawa, The PD-1 expression balance between effector and regulatory T cells predicts the clinical efficacy of PD-1 blockade therapies, Nat. Immunol. 21 (2020) 1346–1358.
[19] T. Kamada, Y. Togashi, C. Tay, D. Ha, A. Sasaki, Y. Nakamura, E. Sato, S. Fukuoka, Y. Tada, A. Tanaka, H. Morikawa, A. Kawazoe, T. Kinoshita, K. Shitara, S. Sakaguchi, H. Nishikawa, PD-1(+) regulatory T cells amplified by PD-1 blockade promote hyperprogression of cancer, Proc. Natl. Acad. Sci. U. S. A. 116 (2019) 9999–10008.
[20] M. Nishi, K. Yoshikawa, J. Higashijima, T. Tokunaga, H. Kashihara, C. Takasu, D. Ishikawa, Y. Wada, M. Shimada, The Impact of Indoleamine 2,3-dioxygenase (IDO) expression on stage III gastric cancer, Anticancer Res. 38 (2018) 3387–3392.
[21] F. Li, Y. Sun, J. Huang, W. Xu, J. Liu, Z. Yuan, CD4/CD8 + T cells, DC subsets, Foxp3, and IDO expression are predictive indictors of gastric cancer prognosis, Cancer Med 8 (2019) 7330–7344.
[22] J.Y. Kim, W.G. Kim, C.H. Kwon, D.Y. Park, Differences in immune contextures among different molecular subtypes of gastric cancer and their prognostic impact, Gastric Cancer 22 (2019) 1164–1175.
[23] D. Kiyozawa, D. Takamatsu, K. Kohashi, F. Kinoshita, S. Ishihara, Y. Toda, M. Eto, Y. Oda, Programmed death ligand 1/indoleamine 2,3-dioxygenase 1 expression and tumor-infiltrating lymphocyte status in renal cell carcinoma with sarcomatoid changes and rhabdoid features, Hum. Pathol. 101 (2020) 31–39.
[24] B.E. Howitt, S.A. Shukla, L.M. Sholl, L.L. Ritterhouse, J.C. Watkins, S. Rodig, E. Stover, K.C. Strickland, A.D. D'Andrea, C.J. Wu, U.A. Matulonis, P. A. Konstantinopoulos, Association of polymerase e-mutated and microsatellite-instable endometrial cancers with neoantigen load, number of tumor-infiltrating lymphocytes, and expression of PD-1 and PD-L1, JAMA Oncol. 1 (2015) 1319–1323.
[25] P. Lauren, The two histological main types of gastric carcinoma: diffuse and so-called intestinal-type carcinoma. An attempt at a histo-clinical classification, Acta Pathol. Microbiol Scand. 64 (1965) 31–49.
[26] R. Inada, S. Sekine, H. Taniguchi, H. Tsuda, H. Katai, T. Fujiwara, R. Kushima, ARID1A expression in gastric adenocarcinoma: clinicopathological significance and correlation with DNA mismatch repair status, World J. Gastroenterol. 21 (2015) 2159–2168.
[27] J.F. Hechtman, S. Rana, S. Middha, Z.K. Stadler, A. Latham, R. Benayed, R. Soslow, M. Ladanyi, R. Yaeger, A. Zehir, J. Shia, Retained mismatch repair protein expression occurs in approximately 6 % of microsatellite instability-high cancers and is associated with missense mutations in mismatch repair genes, Mod. Pathol. 33 (2020) 871–879.
[28] K. Polom, L. Marano, D. Marrelli, R. De Luca, G. Roviello, V. Savelli, P. Tan, F. Roviello, Meta-analysis of microsatellite instability in relation to clinicopathological characteristics and overall survival in gastric cancer, Br. J. Surg. 105 (2018) 159–167.
[29] Y. Kubota, A. Kawazoe, A. Sasaki, S. Mishima, K. Sawada, Y. Nakamura, D. Kotani, Y. Kuboki, H. Taniguchi, T. Kojima, T. Doi, T. Yoshino, G. Ishii, T. Kuwata, K. Shitara, The impact of molecular subtype on efficacy of chemotherapy and checkpoint inhibition in advanced gastric cancer, Clin. Cancer Res 26 (2020) 3784–3790.
[30] A. Tajima, M.T. Hess, B.L. Cabrera, R.D. Kolodner, J.M. Carethers, The mismatch repair complex hMutS alpha recognizes 5-fluorouracil-modified DNA: implications for chemosensitivity and resistance, Gastroenterology 127 (2004) 1678–1684.
[31] D.J. Sargent, S. Marsoni, G. Monges, S.N. Thibodeau, R. Labianca, S.R. Hamilton, A.J. French, B. Kabat, N.R. Foster, V. Torri, C. Ribic, A. Grothey, M. Moore, A. Zaniboni, J.F. Seitz, F. Sinicrope, S. Gallinger, Defective mismatch repair as a predictive marker for lack of efficacy of fluorouracil-based adjuvant therapy in colon cancer, J. Clin. Oncol. 28 (2010) 3219–3226.